INFECTION AND IMMUNITY, Sept. 2008, p. 4269–4281 Vol. 76, No. 9
0019-9567/08/$08.00+0 doi:10.1128/IAI.01735-07

A *Mycobacterium tuberculosis* Rpf Double-Knockout Strain Exhibits Profound Defects in Reactivation from Chronic Tuberculosis and Innate Immunity Phenotypes[▽]

Eleanor Russell-Goldman,[2] Jiayong Xu,[1] Xiaobing Wang,[1] John Chan,[1,2] and JoAnn M. Tufariello[1]*

Departments of Medicine[1] and Microbiology and Immunology,[2] Albert Einstein College of Medicine, Bronx, New York 10461

Received 26 December 2007/Returned for modification 14 February 2008/Accepted 16 June 2008

Resuscitation-promoting factors (Rpfs), apparent peptidoglycan hydrolases, have been implicated in the reactivation of dormant bacteria. We previously demonstrated that deletion of *rpfB* impaired reactivation of *Mycobacterium tuberculosis* in a mouse model. Because *M. tuberculosis* encodes five Rpf paralogues, redundant functions among the family members might obscure *rpf* single-knockout phenotypes. A series of *rpf* double knockouts were therefore generated. One double mutant, Δ*rpfAB*, exhibited several striking phenotypes. Consistent with the proposed cell wall-modifying function of Rpfs, Δ*rpfAB* exhibited an altered colony morphology. Although Δ*rpfAB* grew comparably to the parental strain in axenic culture, in vivo it exhibited deficiency in reactivation induced in C57BL/6 mice by the administration of nitric oxide synthase inhibitor (aminoguanidine) or by $CD4^+$ T-cell depletion. Notably, the reactivation deficiency of Δ*rpfAB* was more severe than that of Δ*rpfB* in aminoguanidine-treated mice. A similar deficiency was observed in Δ*rpfAB* reactivation from a drug-induced apparently sterile state in infected $NOS2^{-/-}$ mice upon cessation of antimycobacterial therapy. Secondly, Δ*rpfAB* showed a persistence defect not seen with the Δ*rpfB* or Δ*rpfA* single mutants. Interestingly, Δ*rpfAB* exhibited impaired growth in primary mouse macrophages and induced higher levels of the proinflammatory cytokines tumor necrosis factor alpha and interleukin 6. Simultaneous reintroduction of *rpfA* and *rpfB* into the double-knockout strain complemented the colony morphology and macrophage cytokine secretion phenotypes. Phenotypes related to cell wall composition and macrophage responses suggest that *M. tuberculosis* Rpfs may influence the outcome of reactivation, in part, by modulating innate immune responses to the bacterium.

Mycobacterium tuberculosis is a globally important human pathogen responsible for an overwhelming burden of disease (10, 12, 64). The pathogen is well suited for its niche within the human host, as the bacterium is able to enter a persistent and possibly dormant state within infected individuals. This clinically silent persistence can continue for decades, until host immune compromise, as by human immunodeficiency virus infection, steroid administration, or senescence, leads to overt disease. Since a significant proportion of the world's population harbors latent tubercle bacilli, understanding latency and reactivation at a molecular level is critical for devising improved strategies for tuberculosis treatment and control.

Our understanding of the latent state remains limited due to both the paucibacillary state associated with tuberculous latency and the inherent difficulties in modeling latent disease. The publication of the complete genome sequence of *M. tuberculosis* (7) has facilitated the study of mycobacterial genes whose homologues in other organisms possess defined functions. Genome-sequencing studies have revealed that *M. tuberculosis* encodes five genes with substantial homology to the resuscitation-promoting factor (Rpf) of *Micrococcus luteus*. The Rpf of *M. luteus* is an ~16- to 17-kDa secreted protein that restores active growth to *M. luteus* cultures rendered "dormant" due to prolonged incubation in stationary phase (36). The Rpf-like proteins of *M. tuberculosis* have also been demonstrated to stimulate the growth of stationary-phase mycobacteria (38). More recently, the Rpf core domain was reported to share structural similarity with both lysozyme and related bacterial peptidoglycan (PG)-degrading enzymes termed lytic transglycosylases, which are involved in metabolism (turnover) of the PG layer of the bacterial cell wall (5, 6). Purified recombinant *M. luteus* Rpf was shown to possess muralytic (PG-degrading) activity on synthetic PG substrates; mutational analysis revealed some correlation between loss of muralytic activity and loss of growth-stimulatory activity (37). It remains unclear how such an enzymatic activity is tied to the resuscitative effects of the Rpfs on dormant bacteria in vitro or in vivo. Possibilities include an alteration of cell wall structure, which overcomes a physical block to cell growth and division (23), versus a more indirect effect through the signaling properties of released cell wall components (PG fragments), which have the potential to signal either within the bacterium or in the mammalian host (13, 18, 19, 32, 49), versus an effect of altered cell wall permeability (24).

The studies described above suggest that *M. tuberculosis* Rpfs can regulate mycobacterial growth. The *rpf*-like genes of *M. tuberculosis* H37Rv are distributed throughout the chromosome, with gene designations Rv0867c (*rpfA*), Rv1009 (*rpfB*), Rv1884c (*rpfC*), Rv2389c (*rpfD*), and Rv2450c (*rpfE*) (http://genolist.pasteur.fr/TubercuList/). We previously found that

* Corresponding author. Mailing address: Division of Infectious Diseases, Department of Medicine, Albert Einstein College of Medicine, Forchheimer Building, Room 406, 1300 Morris Park Avenue, Bronx, NY 10461. Phone: (718) 430-2679. Fax: (718) 430-8725. E-mail: tufariel@aecom.yu.edu.

▽ Published ahead of print on 30 June 2008.

deletion of individual *rpf* genes from the chromosome of *M. tuberculosis* yielded viable mutants showing normal growth and persistence in vitro or in vivo in a mouse model of chronic *M. tuberculosis* infection (60). Using a murine persistent-tuberculosis model in which reactivation was induced by administration of the nitric oxide synthase (NOS) inhibitor aminoguanidine (AG), we found that mice infected with one of the *rpf* deletion mutants—the Δ*rpfB* knockout—displayed a deficiency in reactivation (61). Given the high degree of homology in the "core domain" among the five *M. tuberculosis* Rpfs, we reasoned that redundancy of function could obscure phenotypes for Rpf loss. In fact, others have shown that an *M. tuberculosis* strain deficient in three *rpf*-like genes, but not one, displayed a growth defect in a mouse model (11). More recently, it has been demonstrated that all five Rpfs can be simultaneously deleted from the *M. tuberculosis* chromosome (21) and that the two quadruple-mutant strains examined for in vivo phenotypes were attenuated for growth in a mouse model (21).

Here, we studied a series of *M. tuberculosis* strains with two *rpf*-like genes simultaneously deleted and found that the Δ*rpfAB* mutant displayed a reactivation deficit in mice even more pronounced than that observed for the Δ*rpfB* mutant. In addition, the Δ*rpfAB* mutant exhibited a deficiency in persistence not observed for the Δ*rpfB* strain. Further, compared to wild-type (wt) *M. tuberculosis* Erdman, the Δ*rpfAB* strain displayed altered colony morphology and elicited a different macrophage cytokine response. Cumulatively, these data suggest that RpfA and RpfB function to modulate innate immune responses to *M. tuberculosis* and that these altered host responses may contribute to the impaired capacity for persistence and reactivation.

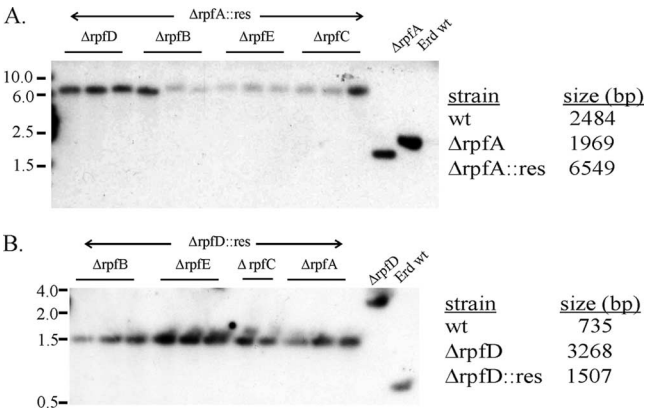

FIG. 1. Southern blots demonstrating the unmarking of the *rpfA* and *rpfD* deletion mutants. (A) Genomic DNAs prepared from putative *rpf* double-knockout strains, from the original single Δ*rpfA* strain, or from Erdman wt were digested with BstEII and probed with a ^{32}P-labeled probe consisting of the upstream flanking region of the *rpfA* gene. The expected band sizes for the Erdman wt, Δ*rpfA*, and Δ*rpfA*::*res* strains are indicated to the right of the blot. (B) Genomic DNAs prepared from putative *rpf* double-knockout strains, from the original single Δ*rpfD* strain, or from Erdman wt were digested with SmaI and probed with a ^{32}P-labeled probe consisting of the upstream flanking region of the *rpfD* gene. The expected band sizes for the Erdman wt, Δ*rpfD*, and Δ*rpfD*::*res* strains are indicated to the right of the blot. Panels A and B show that, for all of the putative double-deletion mutants, the original "parental" strain did possess an unmarked (or "resolved" [*res*]) *rpfA* gene (A) or *rpfD* gene (B). The positions of size markers (kb) are shown on the left of each panel.

MATERIALS AND METHODS

Bacterial strains and growth conditions. The wt *M. tuberculosis* Erdman strain (Trudeau Institute, Saranac Lake, NY) and the various *rpf* gene double-deletion mutants were grown at 37°C in Middlebrook 7H9 broth medium supplemented with 0.2% glycerol, 0.05% Tween 80, and 10% oleic acid-albumin-dextrose-catalase (OADC) enrichment (Becton Dickinson) (complete 7H9 medium), while the solid medium was 7H10 agar supplemented with 0.5% glycerol and 10% OADC (complete 7H10 agar). For growth of the deletion mutants, the medium was supplemented with hygromycin (Roche) at 50 μg/ml.

Construction of *rpf* double-deletion mutants. The construction of the *rpf* single-deletion mutants was described previously (60). To construct the *rpf* double mutants, the Δ*rpfA* and Δ*rpfD* strains were first unmarked by removal of the hygromycin resistance gene. As described previously (1), the specialized *res-hyg-res* gene cassette employed to make the *rpf* knockouts contains the specific DNA binding sites (*res*) for a site-specific γδ-resolvase, the product of the *tnpR* gene of *Escherichia coli* transposon Tn*1000* (Amp^r) (2, 44). Excision of the hygromycin resistance cassette was achieved by transient expression of the γδ-resolvase from the pYUB870 plasmid, with subsequent loss of the *sacB*-expressing pYUB870 plasmid selected for by plating onto medium containing sucrose (1). The second *rpf* deletions were introduced into the Δ*rpfA*::*res* and Δ*rpfD*::*res* unmarked strains by again using the phage-mediated method of specialized transduction (1). Southern blot analysis of the resulting strains is shown in Fig. 1 (demonstrating unmarking of *rpfA* or *rpfD* to generate Δ*rpfA*::*res* and Δ*rpfD*::*res*) and Fig. 2 (demonstrating introduction of the second *rpf* deletions into the unmarked strains). The double-deletion mutants generated were Δ*rpfA*::*res* Δ*rpfB*::*res-hyg-res* (abbreviated Δ*rpfAB*), Δ*rpfA*::*res* Δ*rpfC*::*res-hyg-res* (abbreviated Δ*rpfAC*), Δ*rpfA*::*res* Δ*rpfD*::*res-hyg-res* (abbreviated Δ*rpfAD*), Δ*rpfA*::*res* Δ*rpfE*::*res-hyg-res* (abbreviated Δ*rpfAE*), Δ*rpfD*::*res* Δ*rpfB*::*res-hyg-res* (abbreviated Δ*rpfBD*), Δ*rpfD*::*res* Δ*rpfC*::*res-hyg-res* (abbreviated Δ*rpfCD*), and Δ*rpfD*::*res* Δ*rpfE*::*res-hyg-res* (abbreviated Δ*rpfDE*).

Colony morphology. To evaluate colony morphology, cultures of the Erdman wt, the Δ*rpfAB* double-mutant strain, or the Δ*rpfAB*-complemented strain (see "Complementation of the Δ*rpfAB* mutant" below) were grown to log phase in complete 7H9 medium (supplemented with 50 μg/ml hygromycin for the mutant or 50 μg/ml hygromycin plus 25 μg/ml kanamycin for the complemented strain), serially diluted, and plated onto complete 7H10 agar in the absence of antibiotics. The plates were incubated at 37°C for ~30 to 35 days prior to photographing of the colonies.

Mouse infections including CFU enumeration. Female C57BL/6 mice (Charles River) aged 10 to 12 weeks were infected by aerosol (In-Tox Products, Albuquerqe, NM) with the *M. tuberculosis* strains as described previously (52). Frozen stocks of the strains were inoculated into 7H9 medium, and cultures were grown to an optical density at 600 nm (OD_{600}) of ~1.0, washed in phosphate-buffered saline containing 0.05% Tween 80 (PBS-T), and diluted in PBS-T to a concentration of 1×10^6 to 2×10^6 cells/ml for aerosolization infection. At various times after infection, mice were sacrificed and portions of the lung, spleen, and liver were homogenized in PBS-T. The tissue bacterial load was determined by plating dilutions onto Middlebrook 7H10 agar (Difco) supplemented with 0.5% glycerol and 10% OADC. For the "modified Cornell model" described in "Reactivation protocols" below, NOS2$^{-/-}$ mice (Jackson; strain 002609) were used.

Reactivation protocols. (i) AG administration. Reactivation from the chronic state of infection was induced in chronically infected C57BL/6 mice by the administration of AG (2.5% [wt/vol] ad libitum in the drinking water, along with 5% glucose to improve the palatability of the NOS inhibitor) beginning at 13 to 18 weeks postinfection (14).

(ii) CD4 depletion. In a separate study, as indicated, reactivation was induced in C57BL/6 mice by depletion of CD4$^+$ T cells. Beginning at 6 months after infection, CD4$^+$ T cells were depleted in vivo by weekly intraperitoneal injection of 0.5 mg of rat anti-CD4 monoclonal antibody GK1.5 (Cellex Biosciences, Inc., National Cell Culture Center) as described previously (n = 10 to 11 mice per group) (53). Similarly infected control mice (n = 10 mice per group) were administered normal rat immunoglobulin G (IgG) (Jackson ImmunoResearch Laboratories). The efficacy of CD4 depletion by this protocol was confirmed by flow cytometric analysis of splenocytes of GK1.5- and control rat IgG-treated mice (~77% reduction in the number of CD4$^+$ T cells relative to rat IgG-treated mice at 54 days posttreatment) (data not shown).

(iii) Modified Cornell model. NOS2$^{-/-}$ mice were infected by aerosol; beginning 16 days postinfection, the mice were administered 0.1 g/liter isoniazid (INH) and 8 g/liter pyrazinamide (PZA), with both drugs provided ad libitum in the drinking water. At the end of treatment (3 months), two mice per group were

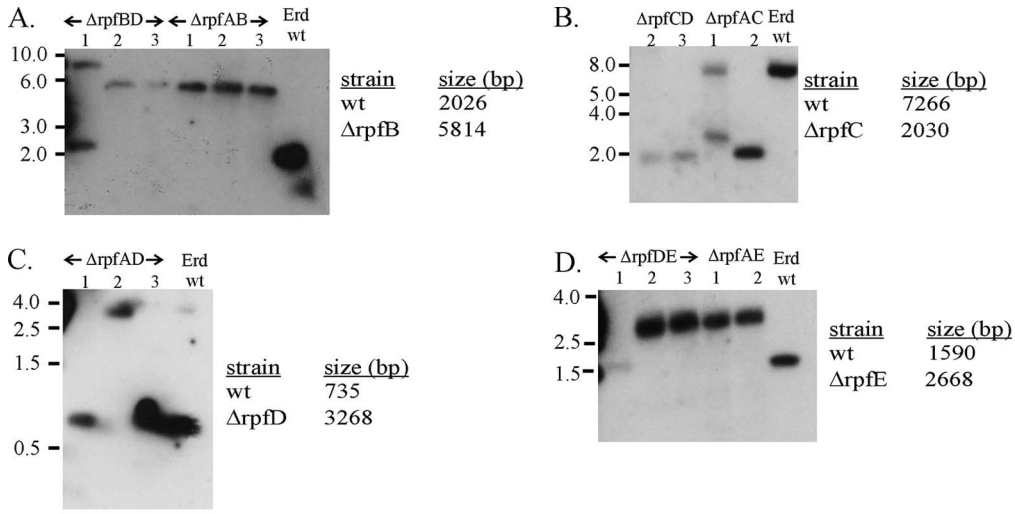

FIG. 2. Southern blots demonstrating that the second *rpf* deletions were introduced into the unmarked Δ*rpfA*::*res* and Δ*rpfD*::*res* strains. Genomic DNAs were digested with SmaI (A and C), BamHI (B), or NcoI (D) and probed with the upstream (B and C) or downstream (A and D) flanking regions of the genes targeted for deletion. The expected band sizes for Erdman wt and the various *rpf* deletion mutants are indicated on the right of each blot. Correct *rpf* double-deletion mutant clones include Δ*rpfBD*-2 and -3 (A), Δ*rpfAB*-1, -2, and -3 (A), Δ*rpfCD*-2 and -3 (B), Δ*rpfAC*-2 (B), Δ*rpfAD*-2 (C), Δ*rpfDE*-2 and -3 (D), and Δ*rpfAE*-1 and -2 (D). The positions of size markers (kb) are shown on the left of each panel.

assessed for tissue sterilization and the remaining mice were observed for disease progression. Mice that were moribund and were judged likely to succumb to the infection within 2 to 3 days were sacrificed and counted as dead.

Growth curves. Starter cultures of the Erdman wt and of the Δ*rpfAB* strain were grown in 10 ml Middlebrook 7H9 medium to an OD_{600} of approximately 1.0 (~3×10^8 to 5×10^8 CFU/ml). A 1-ml aliquot of each culture was pelleted by centrifugation, washed in PBS-T, sonicated to disrupt clumps, and used to inoculate Middlebrook 7H9 medium supplemented with 0.2% glycerol, 0.05% Tween 80, and 10% OADC enrichment to give a final concentration of ~2×10^6 CFU/ml. The inoculum was also serially diluted in PBS-T and plated onto complete 7H10 agar so that the precise number of input CFU could be calculated. The cultures were grown in 250-ml sterile disposable Erlenmeyer flasks (Corning catalogue number 430183) with gentle shaking at 37°C. Aliquots were removed at various times and sonicated; a portion was used to measure the OD_{600}, and the remainder was serially diluted and plated to determine CFU/ml.

Macrophage infections. Bone marrow-derived macrophages were prepared from C57BL/6 mice by flushing isolated femurs with Dulbecco modified Eagle medium (DMEM) (Cellgro) supplemented with 10% heat-inactivated fetal bovine serum, 2 mM L-glutamine, and 1× nonessential amino acids (complete DMEM). The cells were washed and cultured for 7 days on petri dishes in complete DMEM, also supplemented with 20% L929-conditioned medium (LCM). After 7 days, the cells were detached using cold 5 mM EDTA (in PBS), washed in complete DMEM, and resuspended in DMEM with 10% LCM. The cells were seeded into wells of either 6-well (1×10^6 cells/well) or 24-well (2.5×10^5 cells/well) plates and permitted to adhere overnight prior to infection. The macrophages were infected with *M. tuberculosis* strains that were grown to mid-log phase, washed, resuspended in complete DMEM, and diluted to the appropriate titers in complete DMEM. The bacteria were added to the wells at a multiplicity of infection (MOI) of 1 or 5. Uninfected control cultures received no mycobacteria. After 4 h of incubation at 37°C to permit bacterial uptake, the cell monolayers were washed two times with PBS to remove extracellular bacteria, following which complete medium with 10% LCM was added back. At various times after infection, the medium was removed to a tube containing sufficient sodium dodecyl sulfate to give a final concentration of 0.025%; the cell monolayers were lysed with 0.025% sodium dodecyl sulfate and combined with the supernatant. The lysates were diluted in PBS-T and plated onto 7H10-OADC-glycerol for determination of bacterial numbers. For evaluation of growth in activated macrophages, the macrophages were first primed for 24 h with 500 U/ml recombinant murine gamma interferon (IFN-γ) (Peprotech), following which *E. coli* lipopolysaccharide (LPS) (serotype 055:B5; Sigma) at 1 μg/ml was added during the 4-h incubation with the *M. tuberculosis* strains. The subsequent washing and replenishment of media were as described above.

Cytokine measurements. Supernatants of macrophage cultures, either uninfected or infected with the indicated *M. tuberculosis* strains, were collected from the macrophages at 24 h postinfection, filtered twice through a 0.22-μm filter, and stored at −20°C. The concentrations of tumor necrosis factor alpha (TNF-α) or interleukin 6 (IL-6) in the supernatants were analyzed using commercial enzyme-linked immunosorbent assay (ELISA) kits (Quantikine; R&D Systems) according to the manufacturer's instructions.

Complementation of the Δ*rpfAB* mutant. Generation of a pMV306 construct harboring the *rpfB* coding sequence driven by the *hsp60* promoter (P_{hsp60}) has been described previously (60). The *rpfA* coding sequence driven by its native promoter (P_{native}) ~543 bp of upstream sequence that included the binding site for the Rv3676 transcription factor belonging to the cyclic AMP receptor protein (CRP) family (47), was then inserted into this construct. The promoter-*rpfA* cassette was amplified from Erdman genomic DNA (using the primer pair rpfA-start [5′ ACG CGT CTC CTA CCT GCG CGA CGG G 3′] and rpfA-end [5′ TCT AGA CGA CGA ATG GGT GGG TTC GG 3′], with the MluI and XbaI restriction sites underlined), and the resulting PCR product was cloned into the pMV306-*hsp60-rpfB* construct using the MluI and XbaI restriction sites. The resulting plasmid was transformed into the Δ*rpfAB* strain; kanamycin-resistant colonies were selected, and the presence of both of the complementing genes (*rpfA* and *rpfB*), integrated at the *attB* site, was confirmed by Southern blot analysis (see Fig. 9A). The designation for the complemented strain (Δ*rpfA*::*res* Δ*rpfB*::*res-hyg-res attB*::P_{native}*rpfA* P_{hsp60}*rpfB*) is abbreviated Δ*rpfAB*-complemented hereafter.

Statistics. Analysis of survival data was carried out using the Kaplan-Meier method, and the log rank test was used to determine the statistical significance of observed survival differences (GraphPad Prism v.4.01; GraphPad Software, California). Where noted, Student's *t* test (two-tailed) was used to determine the statistical significance for cytokine data and for CFU data (using log-transformed CFU values). For macrophage growth data and for cytokine experiments that included the complemented strain, a one-way analysis of variance (ANOVA) was performed when three or more groups were compared (GraphPad Prism v.4.01; GraphPad Software, California).

RESULTS

Construction of multi-*rpf* knockouts. The vector used to generate the *rpf*-like gene deletion mutants was designed to contain recognition sites for the transposon γδ-resolvase (*res* sites) flanking the hygromycin resistance cassette. We took

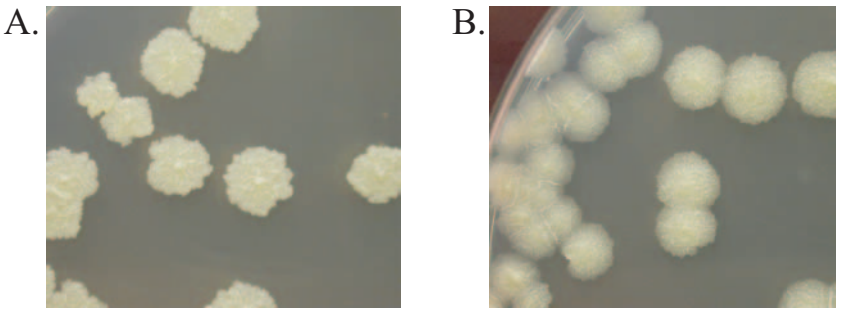

FIG. 3. Δ*rpfAB* exhibits altered colony morphology. Colonies of Δ*rpfAB* (B) are smoother and more regular than those of the Erdman wt strain (A); the Δ*rpfAB* colonies also have a more prominent translucent "halo."

advantage of this vector design to "unmark" the *rpfA* deletion mutant as described previously (1); we have since used the same methods to unmark the *rpfD* mutant, as well. The unmarked strains were used as the substrates to generate mutants with deletion of a second *rpf* gene by specialized transduction. The double knockouts were examined by Southern blotting (Fig. 1 and 2); as expected, all carried a "resolved" version of the gene originally deleted, either *rpfA* or *rpfD* (Fig. 1A and B). The double knockouts obtained were Δ*rpfAB*, Δ*rpfBD*, Δ*rpfAC*, Δ*rpfCD*, Δ*rpfAD*, Δ*rpfAE*, and Δ*rpfDE* (Fig. 2A to D).

Colony morphology. Because Rpfs have homology to lytic transglycosylases, we were interested in the impact *rpf* deletion might have on bacterial cell wall structure, which might be manifested by a colony morphology phenotype. It was therefore notable that, alone among the seven *rpf* double-deletion mutants, the Δ*rpfAB* mutant displayed a distinctly altered colony morphology. Colonies of the Δ*rpfAB* strain were noted to be more circular (with a less irregular border) and smoother (less wrinkled) than colonies of the parental Erdman wt strain; the double mutant also showed a dense central region surrounded by a prominent translucent "halo," giving the colonies a target-like appearance (Fig. 3A and B).

The *rpf* double mutants with disruption of the *rpfB* gene exhibit marked delays in AG-induced mortality in mice. We showed previously that the *M. tuberculosis rpfB* single mutant was significantly delayed in AG-induced reactivation in C57BL/6 mice (61). The seven *rpf* double mutants generated for this study were evaluated for defects in reactivation using the same model. The results showed that only the Δ*rpfAB* and Δ*rpfBD* strains exhibited a marked delay in disease recrudescence, as assessed by mortality (Fig. 4A). None of the mutants with an intact *rpfB* gene displayed the reactivation phenotype. The median survival time (MST) after the start of AG administration was 69 days for Erdman-infected mice and 153 days for Δ*rpfBD*-infected mice but could not be calculated for Δ*rpfAB*-infected mice, because only 2 of 12 mice had succumbed at the time the experiment was terminated after 156 days of AG treatment. The survival curves for Erdman-infected and Δ*rpfAB*-infected mice were significantly different ($P < 0.0001$), as were the curves for Erdman-infected and Δ*rpfBD*-infected mice ($P = 0.0005$). It was apparent that the Δ*rpfAB* and Δ*rpfBD* strains exhibited a more pronounced AG-induced reactivation phenotype than the previously reported Δ*rpfB* single knockout (MST, ~97 to 112 days) (61). Since the Δ*rpfAB* mutant exhibited the most severe reactivation phenotype, we focused on characterizing the in vivo progression of disease caused by this strain.

The Δ*rpfAB* mutant is attenuated in vivo, displaying both a persistence and a reactivation defect. Our previous studies have shown that in C57BL/6 mice, the deletion of any single *rpf* gene from *M. tuberculosis* resulted in no observable defect in growth or persistence through 16 weeks postinfection (60). Analysis of the in vivo growth kinetics of the Δ*rpfAB* strain following pulmonary infection via aerosol, to mimic the most common route of infection, showed that the early growth and

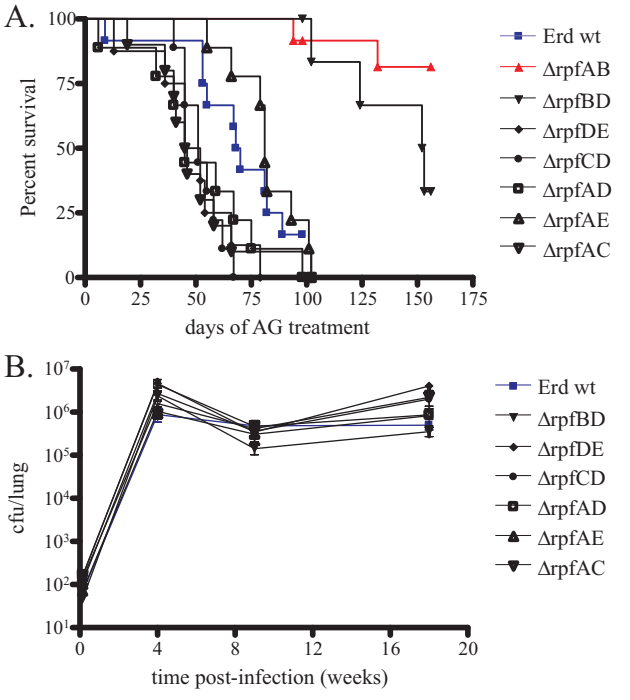

FIG. 4. Δ*rpfAB* and Δ*rpfBD* strains are reactivation deficient. (A) Mortality. C57BL/6 mice were infected with ~100 CFU of *M. tuberculosis* Erd wt or the indicated *rpf* double-deletion mutant: Δ*rpfAB*, Δ*rpfBD*, Δ*rpfDE*, Δ*rpfCD*, Δ*rpfAD*, Δ*rpfAE*, or Δ*rpfAC*. Reactivation was induced at 18 weeks postinfection by AG administration, with survival monitored over time ($n = 8$ to 12 mice per group). (B) Lung titers. C57BL/6 mice were infected by aerosol with the indicated strains, and mice were sacrificed at various time points to determine the numbers of CFU in the lung ($n = 3$ mice per group). The error bars indicate standard errors.

dissemination of the Δ*rpfAB* mutant was unimpaired, with 3-week bacterial numbers nearly identical to those of the Erdman strain in all three organs (Fig. 5). However, by 8 weeks after infection, the lung bacterial burden was ~7-fold lower for the Δ*rpfAB* strain than for the Erdman strain, a difference that increased to 20-fold by 12 weeks postinfection (Fig. 5A). Bacterial numbers in the spleen were also three- to fourfold lower for the Δ*rpfAB* strain than for the Erdman strain at 8 and 12 weeks postinfection, while liver numbers were ~1 log unit lower for the Δ*rpfAB* strain than for the Erdman strain at 12 weeks postaerosol infection (Fig. 5B and C). The CFU differences were maintained at these approximate levels for up to 7 months (data not shown). Two repeat studies demonstrated comparable results. This persistence defect is a unique feature of the *rpfAB* combined knockout, as it was not observed with either the single Δ*rpfA* or Δ*rpfB* mutant (60) or any of the other six double-knockout strains in pulmonary tissue (Fig. 4B).

The in vivo growth kinetics experiments were carried through to examine the reactivation capacity, following pulmonary infection, of the Δ*rpfAB* strain in detail. The results revealed that while the Erdman-infected mice began to exhibit characteristic signs of illness (cachexia, poor coat condition, hunched posture, and decreased mobility) at 11 to 12 weeks after initiation of the NOS inhibitor treatment, mice infected with the double mutant appeared healthy. The numbers of Erdman bacteria recovered from lung and spleen began to rise substantially at this time (Fig. 5), eventually reaching titers of $>10^8$ CFU in the lungs (Fig. 5A) and close to 10^6 in the spleens (Fig. 5B). For the Δ*rpfAB* strain, in contrast, there was little increase in the pulmonary bacterial burden during the period of AG administration (the number of CFU remained $<10^6$) and no increase in the spleen (Fig. 5A and B). After 12 weeks of AG administration, the bacterial burden in Erdman-infected mice had increased by ~10-fold in the liver, while liver bacterial numbers for Δ*rpfAB*-infected mice remained relatively constant during this time interval (Fig. 5C). We note that the difference between the tissue bacterial loads of the Erdman and Δ*rpfAB* strains at some time points late in the course of AG treatment did not reach statistical significance ($P < 0.05$), despite the apparently large differences in the mean values of the data (Fig, 5 A to C). This was most likely due to the large variance introduced by the very high postreactivation CFU values in the Erdman-infected mice, as well as the fact that the mice examined were at different stages in the reactivation process due to an inherent variability in the pace of reactivation in individual mice (see the mortality curves in Fig. 4A and 5D). For example, at 18 weeks of AG administration (31 weeks postinfection), total lung CFU values were 4.8×10^8 and 2.0×10^7 in two Erdman-infected mice versus 1.6×10^5 and 6.8×10^5 in two Δ*rpfAB*-infected mice ($P = 0.08$ by Student's *t* test of log-transformed values).

In agreement with the first study (Fig. 4), the Δ*rpfAB* strain exhibited marked delay in mortality upon AG-induced reactivation. While three of the eight Δ*rpfAB*-infected mice remained alive after >300 days of AG treatment (MST, 307 days), the majority of the 13 Erdman-infected mice had succumbed between days 80 and 125 (MST, 99 days). The mortality curves for the two groups were significantly different ($P = 0.0001$ by the log rank test). Subsequent examination of the long-term survivors in the AG-treated, Δ*rpfAB*-infected group

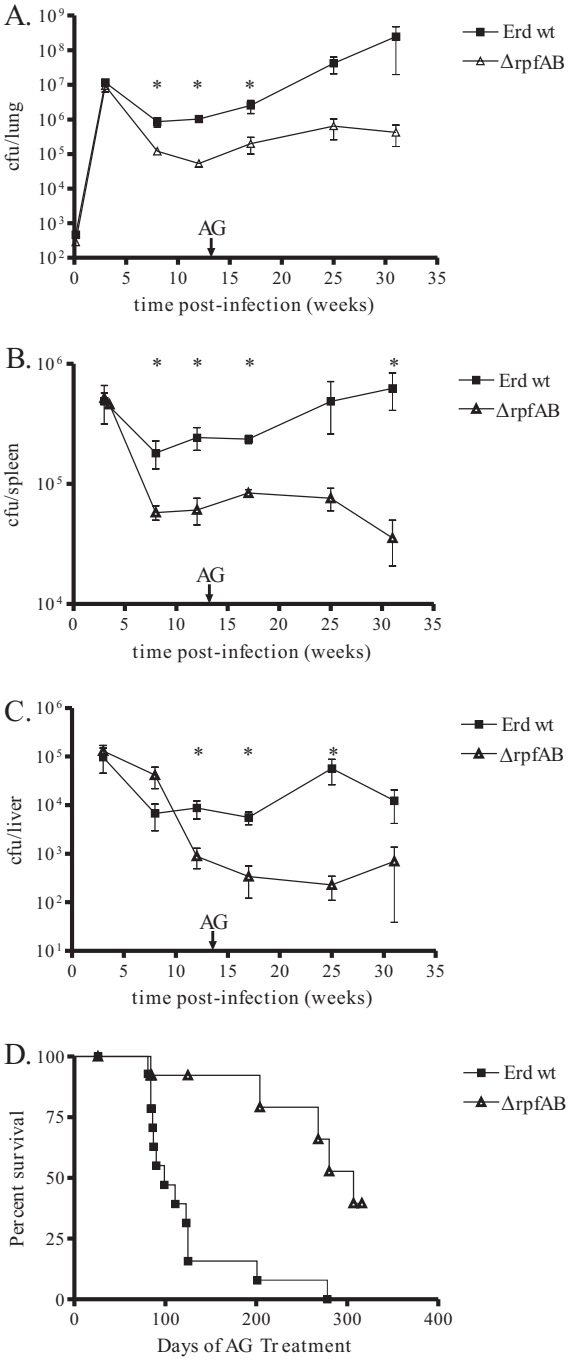

FIG. 5. Δ*rpfAB* is impaired in both persistence and AG-induced reactivation. (A to C) Organ bacterial burdens. C57BL/6 mice were infected by aerosol with ~400 CFU of the Erd wt or Δ*rpfAB* strain, and bacterial counts in the lung (A), spleen (B), and liver (C) were monitored over time ($n = 3$ or 4 mice per time point, except for the final time point, where $n = 2$). The error bars indicate standard errors. (D) Mortality. To induce reactivation, mice were given AG at 13 weeks postinfection as described in Materials and Methods, and survival was monitored. $n = 13$ for the Erd strain and 8 for the Δ*rpfAB* strain. *, *P* value for the Erd strain versus the Δ*rpfAB* strain, <0.05.

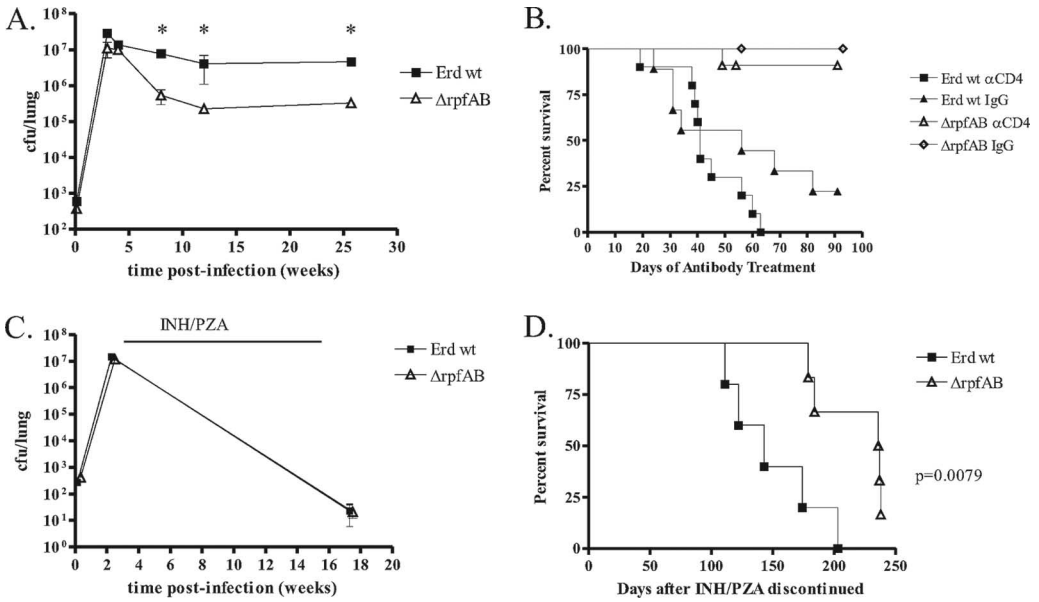

FIG. 6. The Δ*rpfAB* strain exhibits delayed reactivation in alternative models, induced by CD4 depletion in immunocompetent mice (A and B) or a modified Cornell model in NOS2$^{-/-}$ mice (C and D). (A) Pulmonary bacterial burden. C57BL/6 mice were infected by aerosol with ~400 to 600 CFU of the Erd wt or the Δ*rpfAB* strain, and the bacterial burden in the lung was monitored over time ($n = 3$ mice per time point). The error bars indicate standard errors. *, P values for the Erd strain versus the Δ*rpfAB* strain, <0.05. (B) Mortality. Erdman-infected or Δ*rpfAB*-infected mice were administered GK1.5 α-CD4 antibody or rat IgG as a control beginning during the chronic persistent phase of infection (6 months postinfection). $n = 9$ to 11 mice per group. (C) Pulmonary bacterial burden. NOS2$^{-/-}$ mice were infected by aerosol with ~250 to 400 CFU of the Erd wt or Δ*rpfAB* strain, and the bacterial burden in the lung was monitored over time ($n = 2$ mice per time point). The period of INH/PZA administration, beginning at 16 days postinfection and continuing for 3 months, is indicated. (D) Mortality. Erdman-infected or Δ*rpfAB*-infected NOS2$^{-/-}$ mice were observed for mortality. The survival curves are significantly different, as indicated. Although the results of a single experiment are shown, the experiment has since been repeated with similar results.

at 330 days posttreatment revealed that they harbored bacilli, albeit in low numbers, in the lungs (average, 2.5×10^5 CFU) and spleen (average, 1.4×10^4 CFU), indicating that although deficient in recrudescent infection, the Δ*rpfAB* strain can survive for extended periods within murine tissues. Together, the results indicate that the Δ*rpfAB* mutant is severely impaired in its ability to resume growth and multiplication when the production of host antimicrobial reactive nitrogen intermediates is inhibited by AG and that this inability correlates with an attenuation of virulence.

The Δ*rpfAB* mutant exhibits the reactivation-deficient phenotype in a CD4$^+$ T-cell depletion model. In order to explore whether the delayed-reactivation phenotype of the Δ*rpfAB* strain is restricted to the AG model, we analyzed the capacity of the mutant to reactivate in mice upon CD4 depletion (53). This model was selected due to its relevance to human immunodeficiency virus infection and because the reactivation accompanying CD4 depletion occurs independently of NOS2 (53). The bacterial growth kinetics were consistent with prior experiments, with no impairment in the initial log linear phase of *M. tuberculosis* growth (the 3-week time point), followed by a decline in the Δ*rpfAB* pulmonary bacterial load to ~1 log unit lower than the Erdman wt, a deficit maintained through 25 weeks postinfection (Fig. 6A). CD4$^+$ T-cell depletion initiated 6 months after infection led to rapid disease progression in the Erdman-infected mice (MST, 41 days); by comparison, the first death among the Δ*rpfAB*-infected group of 11 mice did not occur until 48 days of anti-CD4 monoclonal antibody GK1.5 treatment (Fig. 6B). The survival curves for Erdman-infected versus Δ*rpfAB*-infected mice treated with GK1.5 were significantly different ($P < 0.0001$) (Fig. 6B). We noted that the Erdman-infected mice receiving rat IgG (MST, 56 days) also exhibited accelerated mortality compared with either of the Δ*rpfAB*-infected groups. This observation was likely due to the fact that the Erdman-infected mice were succumbing to a spontaneous reactivation process unrelated to the administration of IgG, as prior studies have established that rat IgG does not alter disease progression in chronic *M. tuberculosis* infection in mice (35, 53). In addition, the deaths in this group occurred at ~30 to 40 weeks postinfection, late time points at which we had observed significant morbidity accompanied by striking elevations in the lung bacterial burden, as well as deaths, among Erdman-infected mice observed during the natural course of infection (data not shown). Therefore, the curve for the GK1.5-treated mice may include deaths due to spontaneous reactivation, as well as those due to CD4 depletion. In any case, the findings demonstrate that the Δ*rpfAB* strain is significantly impaired in the recrudescence of infection and that the phenotype is a more general phenomenon not restricted solely to the setting of NOS2 inhibition.

The Δ*rpfAB* mutant exhibits delayed reactivation in NOS2$^{-/-}$ mice in a "modified Cornell model" in which prereactivation bacterial numbers are similar to those of the wt. The data presented provide clear evidence for a striking deficiency in the capacity of the Δ*rpfAB* strain to reactivate from a chronic infection. However, since the strain also exhibits a persistence defect, which caused prereactivation organ bacterial numbers to be significantly lower than for the wt (Fig. 5 and 6), inter-

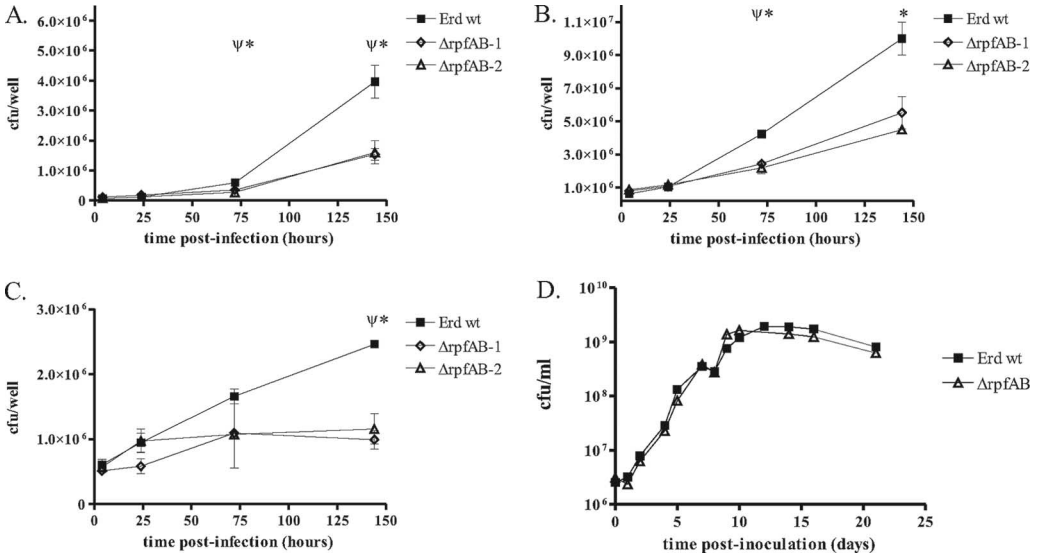

FIG. 7. The Δ*rpfAB* strain is attenuated for growth within macrophages. (A and B) Resting macrophages. Bone marrow-derived macrophages (BMDM) from C57BL/6 mice were infected with Erdman wt, Δ*rpfAB* clone 1 (Δ*rpfAB*-1), or Δ*rpfAB* clone 2 (Δ*rpfAB*-2) at an MOI of 1 (A) or 5 (B), and bacterial numbers were monitored at the indicated time points. (C) Activated macrophages. C57BL/6 BMDM, which had been activated with IFN-γ and LPS, were infected with Erdman wt, Δ*rpfAB* clone 1, or Δ*rpfAB* clone 2, and bacterial numbers were assessed as described above. For panels A, B, and C: ψ, *P* values for the Erd strain versus the Δ*rpfAB*-1 strain, < 0.05; ∗, *P* values for the Erd strain versus the Δ*rpfAB*-2 strain, <0.05. The error bars indicate standard errors. (D) Axenic culture. Growth of the Erd wt and the Δ*rpfAB* strain was monitored in 7H9 medium.

pretation of the reactivation phenotype is not straightforward. To circumvent the potentially confounding factor of the difference in the tissue bacterial burdens in the Δ*rpfAB*- and wt Erdman-infected mice at the onset of reactivation, we employed a modified Cornell model, which involved treating infected mice with antimycobacterial agents for 3 months to achieve an apparently sterile state as previously described by McCune et al. (30, 31). Unlike the original Cornell model, however, but similar to more recently described variations of the model (51), we allowed an initial period of bacterial growth to permit at least partial induction of host immunity prior to initiating the chemotherapy. Rather than using immunocompetent C57BL/6 mice, we infected NOS2$^{-/-}$ mice, as these mice exhibit greatly enhanced susceptibility to *M. tuberculosis* infection (27) and we reasoned that discontinuing INH/PZA treatment in the animals would permit the recrudescence of infection in a manner analogous to administration of NOS inhibitors to chronically infected wt mice (14, 27).

In the NOS2$^{-/-}$ mouse, growth of both the Erdman wt and the Δ*rpfAB* strain in the lungs after a low-dose aerogenic challenge was rapid, achieving lung titers of $\sim 10^7$ CFU at 16 days postinfection (Fig. 6C). The INH/PZA treatment was begun at this time and continued for 3 months. The total numbers of lung CFU were very low (<50) and were similar for the two strains when assessed at 2 weeks after drug discontinuation (Fig. 6C); viable mycobacteria were not recovered from the spleen or liver at this time point. In a separate experiment (not shown), no mycobacteria were recovered from lung, spleen, or liver homogenates when the organs were harvested at a slightly earlier time point, 2 days following drug discontinuation, indicating that the apparently sterile state had been achieved with our model. Even with this "equalization" of the prereactivation pulmonary bacterial numbers, NOS2$^{-/-}$ mice infected with the Δ*rpfAB* strain still exhibited significantly delayed mortality compared with Erdman-infected mice ($P = 0.0079$ by the log rank test) (Fig. 6D). The median survival after drug discontinuation was 143 days for Erdman wt-infected mice versus 237 days for those infected with the Δ*rpfAB* strain. The results demonstrate that the deficiency in growth resumption during chronic infection is separable from the lower prereactivation CFU "set point" and echo our earlier findings with the Δ*rpfB* single mutant, which exhibited delays in reactivation in the absence of any persistence defect (61). This experiment also provides further evidence that the reactivation defects observed for the *rpf* mutants are not confined to the AG-induced reactivation model but are seen in a variety of in vivo contexts where the bacteria recrudesce from a persistent state.

The Δ*rpfAB* mutant has an attenuated phenotype in both unactivated and activated macrophages. Macrophages are important in vivo targets for *M. tuberculosis* infection. An array of *M. tuberculosis* mutants with altered virulence, including some with altered cell wall structure, have been found to exhibit changes in their capacities to modulate host immune responses in macrophage systems (25, 28, 29, 42, 43, 55, 57). Given the distinct colony morphology of the Δ*rpfAB* mutant and the in vivo attenuation relative to the Erdman strain, we reasoned that the interactions of the Δ*rpfAB* strain with macrophages might be altered and chose to characterize these further in an ex vivo bone marrow-derived macrophage system. Growth of the Erdman wt and of two independently obtained clones of the Δ*rpfAB* double mutant (Δ*rpfAB*-1 and Δ*rpfAB*-2) was assessed over a 6-day period. Uptake levels at 4 h were similar for the wt and Δ*rpfAB* double-mutant strains, but both of the Δ*rpfAB* clones (1 and 2) displayed diminished growth in unactivated macrophages, with approximately twofold fewer CFU by day 6 (Fig. 7A and B). An intracellular growth defect for

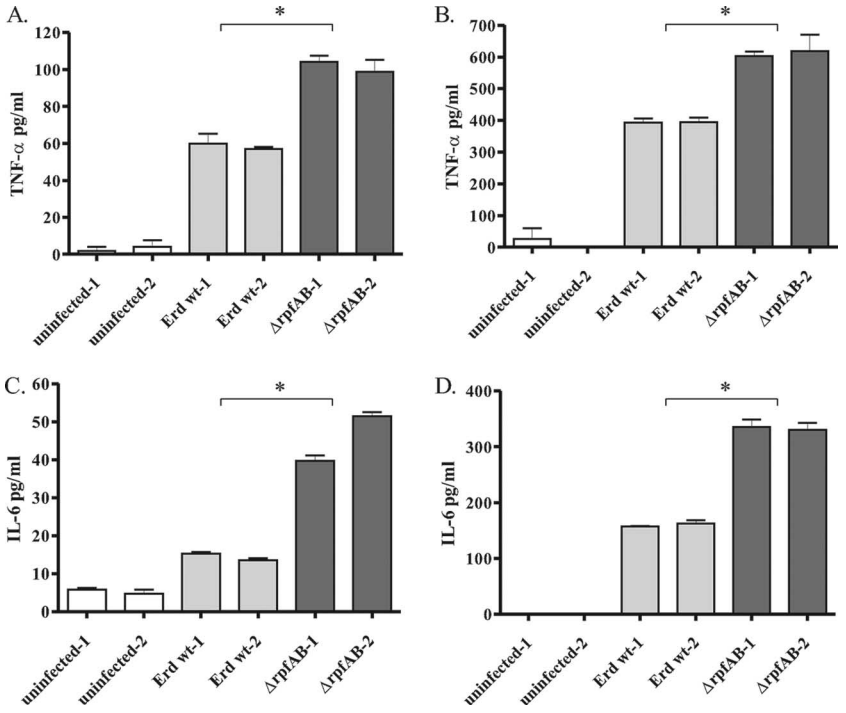

FIG. 8. The Δ*rpfAB* strain induces increased macrophage production of TNF-α and IL-6. C57BL/6 BMDM were infected with Erdman wt (light-gray bars) or Δ*rpfAB* clone 2 (dark-gray bars) at an MOI of 1 (A and C) or 5 (B and D) or left uninfected (white bars). Supernatants collected at 24 h were assayed for TNF-α (A and B) or IL-6 (C and D) by ELISA. The results of representative experiments are shown. Samples from each well were assayed in duplicate, and the results are shown as means plus standard errors. The designations Erd-1 and -2 and Δ*rpfAB*-1 and -2 refer to each of the two samples assayed for each experiment shown. *, *P* for the Erdman versus the Δ*rpfAB* strain, <0.05.

Δ*rpfAB* clones 1 and 2 was also found for macrophages stimulated with IFN-γ and LPS (Fig. 7C), where the growth of the Erdman wt was suppressed compared with unactivated macrophages but the mutants displayed even greater growth suppression, with nearly flat growth curves from day 1 to day 6. The results suggest a role for RpfA and -B in promoting mycobacterial growth in resting macrophages and possibly mycobacterial persistence/survival in activated macrophages. In contrast to the macrophage growth findings, the Δ*rpfAB* strain did not show a significant growth defect when propagated in broth media (Fig. 7D).

Macrophages infected with the Δ*rpfAB* mutant produce higher levels of the proinflammatory cytokines TNF-α and IL-6. To evaluate the contributions of *rpfA* and *rpfB* expression to the modulation of host immune responses, we compared levels of TNF-α and IL-6 secretion in C57BL/6 bone marrow-derived macrophages infected with the Δ*rpfAB* mutant and the Erdman wt at 24 h postinfection. These cytokines were chosen because preliminary analysis of multiple cytokines using a cytometric bead assay (Millipore Beadlyte Mouse Multi-Cytokine Detection System 2) (data not shown) had revealed that they were the most vigorously induced cytokines in our system, while the 24-h time point was selected because CFU values for the wt and mutant were very similar, eliminating bacterial numbers as a variable in cytokine induction. Macrophages infected with the Δ*rpfAB* strain (clone 2 was used in these studies) produced greater amounts of both TNF-α and IL-6 than those infected with the Erdman wt, with average differences just under 2-fold for TNF-α and 2.5- to 3-fold for IL-6 (Fig. 8A to D). The results suggest that absence of *rpfA* and *rpfB* renders the mutant more proinflammatory in terms of macrophage TNF-α and IL-6 production. Therefore, the Rpfs, perhaps through their activities on the mycobacterial cell wall, may play a role in host immune evasion.

Complementation of the colony morphology and the macrophage cytokine secretion phenotypes. In order to complement the Δ*rpfAB* mutant, single copies of the *rpfA* and *rpfB* coding sequences were introduced into the double-knockout strain at the *attB* site (Fig. 9A); expression of both genes was confirmed in log-phase bacteria using real-time reverse transcription-PCR analysis (data not shown). Comparison of the colony morphology of the Δ*rpfAB*-complemented strain to that of the Erdman wt and the Δ*rpfAB* strains demonstrated a clear conversion of the complemented strain away from the circular and smoother morphology of the Δ*rpfAB* strain, so that the complemented strain colonies were nearly indistinguishable from those of the Erdman wt, often actually exhibiting a rougher, more wrinkled appearance than the wt strain (Fig. 9B). This observation is consistent with the view that the Δ*rpfAB* strain exhibits RpfA/RpfB-dependent cell wall structural changes. The macrophage phenotypes of the complemented strain were also assessed. Strikingly, the enhanced cytokine secretion phenotype seen with the Δ*rpfAB* strain was reversed in the complemented strain (Fig. 9C). In the experiment shown, the macrophages were infected at an MOI of 5, and the supernatants were harvested for cytokine analysis at 24 h postinfection. When the data were analyzed by one-way ANOVA, production of both TNF-α and IL-6 was found to be significantly

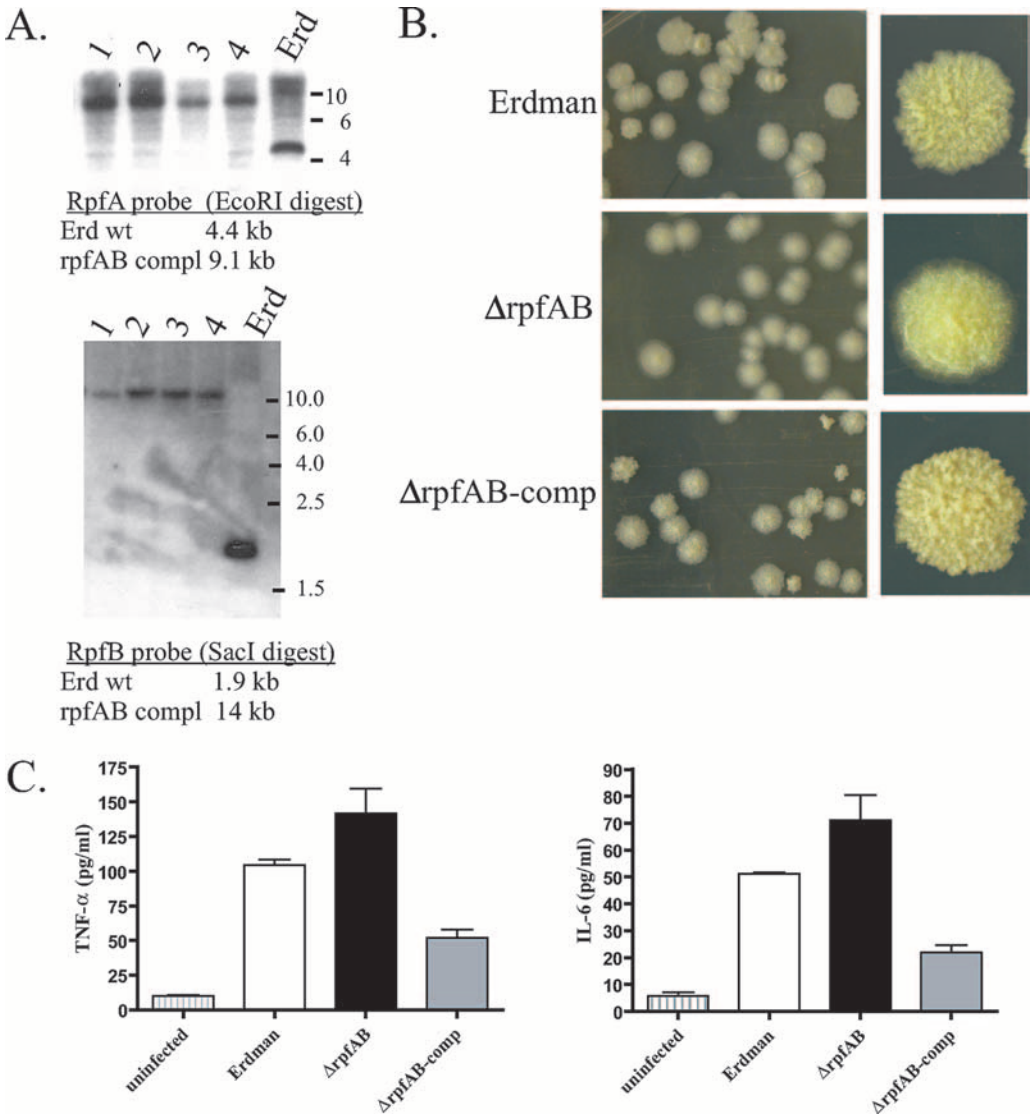

FIG. 9. Complementation of the Δ*rpfAB* strain with combined expression of *rpfA* and *rpfB* restores the wt colony morphology and reduces the macrophage proinflammatory cytokine stimulation toward wt levels. (A) Southern blots demonstrating the presence of the *rpfA* and *rpfB* genes inserted at the *attB* site of the Δ*rpfAB*-complemented (compl) strain. Genomic DNAs prepared from putative Δ*rpfAB*-complemented strains (clones 1 to 4) or from Erdman wt were digested with EcoRI (top) or SacI (bottom) and probed with a ^{32}P-labeled probe consisting of *rpfA* coding sequences (top) or *rpfB* coding sequences (bottom). The expected band sizes for the Erdman wt and for the Δ*rpfAB*-complemented strain are indicated below each blot. The positions of size markers (kb) are shown to the right of each blot. (B) Colonies of the Δ*rpfAB*-complemented (comp) strain (bottom) are rougher/more wrinkled than those of the Δ*rpfAB* parental strain (middle) and more closely resemble the rough colonies of the Erdman wt strain (top). Shown are plates with numerous colonies (similar in number) on the left and a single large colony from a sparsely inoculated plate containing only a few colonies in total on the right. (C) Production of TNF-α and IL-6 by macrophages infected with the Erdman wt, Δ*rpfAB*, and Δ*rpfAB*-complemented strains. C57BL/6 bone marrow-derived macrophages were left uninfected (vertically hatched bars) or were infected with the Erdman wt (white bars), Δ*rpfAB* (black bars), or Δ*rpfAB*-complemented (gray bars) strain at an MOI of 5; the supernatants collected at 24 h were assayed for TNF-α (left) or IL-6 (right) by ELISA. The results of a representative experiment are shown. The results are shown as means plus standard errors of two individual samples per treatment group (with each sample assayed in duplicate).

lower ($P < 0.05$) for macrophages infected with the Δ*rpfAB*-complemented strain than for macrophages infected with the parental Δ*rpfAB* strain. Although in this experiment the differences between the remaining infected groups did not reach the level of statistical significance ($P > 0.05$ by one-way ANOVA), the trend toward enhanced production of TNF-α and IL-6 elicited by infection with the Δ*rpfAB* strain compared with the Erdman wt was again observed. Although results of a representative experiment are shown, the trend toward lower TNF-α and IL-6 induction by the Δ*rpfAB*-complemented strain than by the Δ*rpfAB* strain was observed in five independent experiments (with MOIs ranging from 1 to 5).

Interestingly, the attenuated intramacrophage growth phenotype of the Δ*rpfAB* strain was not reversed in the complemented strain (data not shown). This demonstrates that the cytokine secretion and macrophage growth phenotypes are separable. The failure of the growth phenotype to be complemented deserves further investigation but could reflect the

inappropriate levels or timing of expression of *rpfA* and/or *rpfB* in the complemented strain.

DISCUSSION

Latency and reactivation are central features of *M. tuberculosis* pathogenesis, but the bacterial factors that regulate these processes are largely unknown. The *M. tuberculosis* Rpfs are of obvious interest in this regard because of their ability to stimulate the growth of late-stationary-phase *Mycobacterium bovis* BCG cultures (36, 38) and our earlier observation that a single *rpfB* knockout displayed a delay in AG-induced reactivation in mice relative to the wt Erdman strain (61). However, although the impact of the single *rpfB* knockout on reactivation was clear, a number of important questions remained regarding the role of Rpfs in *M. tuberculosis* reactivation. These questions include whether the five *M. tuberculosis* Rpfs possess redundant functions relevant to bacterial growth, persistence, and reactivation.

The present study reinforces the role of RpfB in regulating *M. tuberculosis* reactivation and implicates RpfA in the same process. The phenotype of the single *rpfB* knockout was delayed reactivation following AG administration, while no defect in bacterial persistence was detected. In the current study, we found that the combined *rpfA*/*rpfB* knockout displayed an even more dramatic impairment in AG-induced reactivation, with Δ*rpfAB*-infected mice exhibiting an extremely prolonged median survival of ~300 days of AG treatment, or ~400 days postinfection. A separate mortality group not treated with AG was not included in this experiment. However, the Δ*rpfAB*-infected, AG-treated (from 3 months onward) mice survived longer than the ~250- to 350-day MSTs for historical C57BL/6 controls infected by aerosol with the Erdman or H37Rv wt strain and allowed to succumb to the natural course of infection (i.e., in the absence of AG administration) (34, 40, 62). Overall, the results indicate an extreme defect for the Δ*rpfAB* strain in reactivation induced by NOS inhibition. As described above, we also observed delayed mortality in a model of reactivation induced by depletion of $CD4^+$ T cells (Fig. 6B), excluding the possibility that the reactivation deficit is specific to the AG system and suggesting a general effect of the Rpfs on growth resumption from a persistent or dormant state. The fact that the phenotype was also observed in the "modified Cornell model" employing $NOS2^{-/-}$ mice (Fig. 6D) indicates that even when the reactivation process commences from similar and extremely low bacterial numbers, the growth resumption of the double mutant is impaired compared with the wt.

The other notable phenotype of the double mutant, compared to the single *rpfB* mutant, is the persistence defect seen with the Δ*rpfAB* strain. The identification of *M. tuberculosis* genes that play critical roles during the chronic phase of infection has been an area of great interest, especially as the gene products may provide targets for drugs designed to abbreviate courses of therapy or for strategies to control reactivation from latent infection. One of the first *M. tuberculosis* mutants found to show a specific defect in persistence was deleted for *pcaA*, which encodes an enzyme responsible for the cyclopropanation of the α-mycolate class of cell wall fatty acids (15). Similar to Δ*rpfAB*, the Δ*pcaA* strain was found to exhibit altered cell surface properties (it was originally identified in a screen for mutants defective in cording); also reminiscent of Δ*rpfAB*, the impact of the *pcaA* deletion on survival was pronounced, despite a relatively modest deficit in the pulmonary bacterial burden during chronic infection (15). The Δ*pcaA* strain was also found to induce altered macrophage inflammatory responses (41). It is difficult to identify overarching themes regarding the mycobacterial factors implicated in persistence in vivo, although a number of *M. tuberculosis* mutants with disruption of genes involved in cell envelope composition (15, 56) and in fatty acid metabolism (33) have been found to display defects in survival at late stages of infection, with the latter association postulated to reflect a shift in the metabolism of persisting organisms toward reliance on fatty acids as sources of energy. As may be expected, if the transition into a persistent state requires significant alterations in gene expression, mutations in various transcriptional regulatory factors have also been associated with impaired persistence (58, 63) or with attenuated virulence impacting host inflammatory responses and time to death without affecting bacterial numbers (22, 59).

It is unclear why the combined *rpfA*/*rpfB* mutant shows a persistence defect that is lacking in the single A and B mutants. As discussed further below, others have also recently reported in vivo attenuation of multi-*rpf* knockout strains in murine models, including defects in persistence (3, 21). In previous work, we did note a trend toward pulmonary bacterial burdens ~2-fold lower in the Δ*rpfB* strain versus the wt; however, although this was a consistent trend, the small difference did not always achieve statistical significance (61). Although the persistence of *M. tuberculosis* within the tissues of chronically infected mice is thought to represent a relatively static equilibrium, it is believed that there is some ongoing slow replication of at least a subset of bacteria occurring at least intermittently, which serves to maintain bacterial numbers (39, 45), albeit with a population doubling time estimated at ~70 days (39). Although speculative, it is possible that the *rpf* mutants are deficient in this ongoing low rate of bacterial replication, perhaps due to cell wall alterations that interfere with cellular division (23). Such a deficiency may be specific to an altered cell wall architecture that occurs during stationary phase/dormancy (9, 26, 54) and therefore may not be apparent during growth under standard in vitro culture conditions or in the acute phase of logarithmic growth in mice. As an alternative (or in addition) to a defect in bacterial division that impairs "replacement" of bacteria eliminated by the host during chronic infection, it is also possible that *rpf* mutants display heightened susceptibility to antimycobacterial host defenses that characterize the chronic phase of infection. That is, the defect may be one that tips the balance toward more rapid or efficient bacterial destruction rather than one that hinders cell division and bacterial replication. In this regard, it would be of interest to examine the susceptibility of the Δ*rpfAB* strain to the killing effects of NO, thought to be a critical antimycobacterial defense of macrophages (4, 20, 27, 46), as well as survival of the mutant under environmental stresses, such as hypoxia and nutrient deprivation, which are thought to be encountered during persistence. Another area that warrants further exploration is the impact that the enhanced proinflammatory cytokine production by infected macrophages has upon the subsequent development of adaptive immune responses, especially

as the in vivo growth attenuation is first apparent at 3 to 4 weeks postinfection, the time of onset of adaptive immunity.

As noted previously, Rpf proteins are thought to possess cell wall-modifying enzymatic activity (5, 6, 37). The solution structure of the *M. tuberculosis* core Rpf domain was recently solved by nuclear magnetic resonance and found to possess similarity to the structure of the c-type lysozymes (CAZy family, GH22) and soluble lytic transglycosylases (CAZy family, GH23) (5). A recent crystallographic analysis of a portion of RpfB (including both the G5 and Rpf core domains) has also been reported, with the best crystals obtained upon cocrystallization with tri-*N*-acetylglucosamine (50). Additionally, purified recombinant His-tagged *M. luteus* Rpf was found to possess muralytic activity, with the capacity to hydrolyze both fluorescamine-labeled *M. luteus* cell walls and the synthetic lysozyme substrate 4-methylumbelliferyl-β-D-*N*,*N*′,*N*″-triacetylchitotrioside, albeit with activity about 1/5 to 1/50 that of hen egg white lysozyme in the various assays (37). Further, mutation of conserved Rpf residues revealed some correlation between loss of muralytic activity and loss of growth-stimulatory activity, although the correlation was imperfect, with some mutations causing substantial impairment of cell wall hydrolytic activity but with minimal effects on culturability (37). Also consistent with a role for Rpfs in modulating cell wall structure, a secreted *M. tuberculosis* cell wall hydrolase that localizes to the septa of actively dividing mycobacteria has recently been identified as a binding partner for RpfB (17). Interestingly, the conserved portion of RpfB alone had minimal capacity to degrade various cell wall substrates, yet this portion of RpfB was able to act in synergy with the cell wall hydrolase previously identified as a binding partner (Rv1477, termed RipA) to enhance the hydrolytic ability of RipA (16). That combined deletion of *rpfA* and *-B* results in altered cell wall structure is suggested by our finding of altered colony morphology for the mutant relative to the parental strain (Fig. 3), a phenotype that was reversed by reintroduction of the *rpf* genes (Fig. 9).

It is not clear why a variety of other double-knockout strains tested did not display colony morphology and reactivation phenotypes similar to the Δ*rpfAB* strain, although differences in the enzymatic activities, specificities, subcellular localization, or timing of expression of the various Rpfs may account for the findings. RpfA and -B are the largest of the *M. tuberculosis* Rpf proteins, each possessing lengthy unique regions in addition to the conserved Rpf domain. RpfA has C-terminal proline- and alanine-rich repeats following the Rpf domain, while RpfB has unique features, including a lipoprotein lipid attachment site and several conserved domains (one G5 and three DUF348) at its N terminus, domains that, although with unknown functions, are hypothesized to play roles in substrate binding (50).

Two recent studies also provide new information regarding the *M. tuberculosis* Rpf function and lend support to the results obtained in our study. As noted above, all of our double Rpf deletions were viable in broth culture. Kana et al. have recently demonstrated that in fact all five *M. tuberculosis* paralogues can be deleted from the *M. tuberculosis* chromosome without adverse effects on growth in broth culture, although colony formation on solid media was delayed in the quintuple and selected quadruple mutants (21). Mutants with deletions of three or more Rpfs also displayed defects in resuscitation from an in vitro "nonculturable" state, but these phenotypes could be at least partially reversed by genetic complementation, strongly suggesting that the phenotypes detected were due to Rpf loss (21). Additionally, Kana et al. provide evidence of in vivo attenuation of Rpf quadruple knockouts (growth and persistence defects) (21), which is consistent with our data showing the deletion of RpfA and -B alone is sufficient to confer an in vivo persistence defect. Going beyond these phenotypes, our data also demonstrate an impact of RpfA and -B upon cytokine production by macrophages and upon reactivation from latent infection following aerosol infection. Our studies clearly demonstrate that the Δ*rpfAB* reactivation defect is not particular to an individual reactivation method and that the simultaneous deletion of RpfA and -B affects not only bacterial titers, but also the outcome of infection as monitored by lethality. Consistent with these conclusions, deletion of Rpfs influenced in vivo bacterial titers following AG-induced reactivation in a nonlethal intraperitoneal-infection model (3).

In regard to in vitro growth phenotypes, we found the Δ*rpfAB* strain to be attenuated for intramacrophage growth, while *M. tuberculosis* quadruple mutants were unimpaired for growth within monocytes (21). Although it is possible that the double mutant may display an intracellular growth phenotype that is reversed by further Rpf deletion, it may be that the discrepant results are attributable to the different macrophage systems employed (of murine versus human origin). The differences could also be attributable to the different *M. tuberculosis* parental strains (Erdman versus H37Rv) used in these studies. For instance, the H37Rv strain used to construct the quadruple mutants was deficient in synthesis of phthiocerol dimycocerosate (PDIM) (21), a phenotype that can alter virulence (8, 48), while the Erdman-derived Δ*rpfAB* strain appears unimpaired in PDIM synthesis (J. Chan and J. M. Tufariello, unpublished data). In contrast to the macrophage cytokine induction phenotype, the attenuated intramacrophage growth was not reversed by complementation despite the fact that two independent clones of the Δ*rpfAB* mutant reliably exhibited this phenotype, suggesting that the observed phenotype was caused by the disruption of *rpfA* and *rpfB*. Reminiscent of this partial complementation is the observation that the in vitro resuscitation of dormant *M. tuberculosis* Rpf quadruple mutants was substantially restored by complementation, while the complementation of in vivo phenotypes was equivocal (with partial growth restoration in some, but not all, mice at early time points and the effect completely absent at later time points) (21). Clearly there are multiple explanations for partial complementation in complex systems involving interactions of bacteria with host cells or organisms, especially when the complementing genes are placed outside of their normal chromosomal contexts and, in some cases, driven by heterologous promoter sequences or arbitrary lengths of upstream sequence that may not represent the full promoter.

Although the Rpf of *M. luteus* was originally referred to as a "bacterial cytokine" (36), the mechanism by which the Rpfs may be influencing reactivation remains uncertain. The demonstration of Rpf enzymatic activity has led to additional or alternative hypotheses, other than loss of a growth-stimulatory factor, that may contribute to the reactivation deficit seen in the present study, including the possibility that Rpfs regulate growth by cleaving components of the cell wall to relieve a block to cell division (23). Another hypothesis that has drawn

less attention is the possibility that alterations in bacterial PG structure may alter host responses to infection and that these altered host responses may underlie the observed in vivo defects in growth, persistence, and reactivation. In the present study, we found that the Δ*rpfAB* mutant exhibited altered interactions with macrophages, inducing higher levels of proinflammatory cytokines. There is accumulating evidence that the regulation of both innate and adaptive immune responses is a critical component of *M. tuberculosis* virulence. A variety of *M. tuberculosis* mutant strains with altered virulence properties, including some with modified cell wall structure, have been found to exhibit changes in their capacities to modulate host immune responses in macrophage systems (25, 28, 29, 42, 43, 55, 57). The Δ*rpfAB* mutant appears to share some features with the mycobacterial *secA2* and *snm* secretion system mutants, both of which show growth defects in cultured macrophages, as well as eliciting increased levels of proinflammatory cytokines (25, 57). This similarity is intriguing, as it raises the possibility that some phenotypes observed for loss of RpfA and -B may be due to altered secretory capacity or cell wall permeability. Although a role for Rpfs in such processes has not been examined, lytic transglycosylases of gram-negative bacteria have been identified as components of various macromolecular transport systems (24).

Overall, our data demonstrate that the dramatic reactivation defect of the Δ*rpfAB* mutant is accompanied by both altered colony morphology and an enhanced ability to stimulate macrophage proinflammatory cytokine production. These results reinforce the proposed cell surface-modifying properties of Rpfs and suggest the possibility that the interaction of a tubercle bacillus with altered surface components might elicit a macrophage immune response distinct from that triggered by wt *M. tuberculosis*. However, we recognize that the in vivo findings, and whether they are directly attributable to combined loss of the *rpf* genes, should be interpreted with some caution, given our inability to fully complement the in vitro phenotypes of the Δ*rpfAB* mutant (that is, the lack of complementation of the macrophage growth defect). However, the fact that others have also found that multi-*rpf* deletion mutants (derived from a different parental strain than our own and studied in mouse model systems that differ from ours in terms of the mouse strain or route of infection) exhibited defects in persistence and in reactivation (3, 21) lends support to the validity of the findings for our Δ*rpfAB* mutant and to a direct causative role for the *rpf* genes in the phenotype. The results are further bolstered by the fact that, in the current study, only double mutants bearing the *rpfB* deletion showed significant reactivation defects, despite the fact that all mutants underwent a similar process of passaging for strain construction. Further investigation into the impact of this important family of proteins on innate immunity and the subsequent ability of the host to control persistent and reactivated tuberculous infection is warranted.

ACKNOWLEDGMENTS

We extend sincere thanks to John Kim for assistance with macrophage preparation and to all members of the Chan laboratory for numerous helpful discussions.

This work was supported by NIH grants AI065313 (J.M.T.) and HL71241 (J.C.). Generous funding was also provided to J.M.T. by the Center for AIDS Research (CFAR) Developmental Core at the Albert Einstein College of Medicine and Montefiore Medical Center (NIH AI51519), by the Potts Memorial Foundation, and by the Stony Wold-Herbert Fund.

REFERENCES

1. **Bardarov, S., S. Bardarov, Jr., M. S. Pavelka, Jr., V. Sambandamurthy, M. Larsen, J. Tufariello, J. Chan, G. Hatfull, and W. R. Jacobs, Jr.** 2002. Specialized transduction: an efficient method for generating marked and unmarked targeted gene disruptions in *Mycobacterium tuberculosis*, *M. bovis* BCG and *M. smegmatis*. Microbiology **148:**3007–3017.
2. **Berg, C. M., N. B. Vartak, G. Wang, X. Xu, L. Liu, D. J. MacNeil, K. M. Gewain, L. A. Wiater, and D. E. Berg.** 1992. The m gamma delta-1 element, a small gamma delta (Tn1000) derivative useful for plasmid mutagenesis, allele replacement and DNA sequencing. Gene **113:**9–16.
3. **Biketov, S., V. Potapov, E. Ganina, K. Downing, B. D. Kana, and A. Kaprelyants.** 2007. The role of resuscitation promoting factors in pathogenesis and reactivation of *Mycobacterium tuberculosis* during intra-peritoneal infection in mice. BMC Infect. Dis. **7:**146.
4. **Chan, J., Y. Xing, R. S. Magliozzo, and B. R. Bloom.** 1992. Killing of virulent *Mycobacterium tuberculosis* by reactive nitrogen intermediates produced by activated murine macrophages. J. Exp. Med. **175:**1111–1122.
5. **Cohen-Gonsaud, M., P. Barthe, C. Bagneris, B. Henderson, J. Ward, C. Roumestand, and N. H. Keep.** 2005. The structure of a resuscitation-promoting factor domain from *Mycobacterium tuberculosis* shows homology to lysozymes. Nat. Struct. Mol. Biol. **12:**270–273.
6. **Cohen-Gonsaud, M., N. H. Keep, A. P. Davies, J. Ward, B. Henderson, and G. Labesse.** 2004. Resuscitation-promoting factors possess a lysozyme-like domain. Trends Biochem. Sci. **29:**7–10.
7. **Cole, S. T., R. Brosch, J. Parkhill, T. Garnier, C. Churcher, D. Harris, S. V. Gordon, K. Eiglmeier, S. Gas, C. E. Barry III, F. Tekaia, K. Badcock, D. Basham, D. Brown, T. Chillingworth, R. Connor, R. Davies, K. Devlin, T. Feltwell, S. Gentles, N. Hamlin, S. Holroyd, T. Hornsby, K. Jagels, B. G. Barrell, et al.** 1998. Deciphering the biology of *Mycobacterium tuberculosis* from the complete genome sequence. Nature **393:**537–544. (Erratum, **396:** 190.)
8. **Cox, J. S., B. Chen, M. McNeil, and W. R. Jacobs, Jr.** 1999. Complex lipid determines tissue-specific replication of *Mycobacterium tuberculosis* in mice. Nature **402:**79–83.
9. **Cunningham, A. F., and C. L. Spreadbury.** 1998. Mycobacterial stationary phase induced by low oxygen tension: cell wall thickening and localization of the 16-kilodalton alpha-crystallin homolog. J. Bacteriol. **180:**801–808.
10. **Dolin, P. J., M. C. Raviglione, and A. Kochi.** 1994. Global tuberculosis incidence and mortality during 1990–2000. Bull. W. H. O. **72:**213–220.
11. **Downing, K. J., V. V. Mischenko, M. O. Shleeva, D. I. Young, M. Young, A. S. Kaprelyants, A. S. Apt, and V. Mizrahi.** 2005. Mutants of *Mycobacterium tuberculosis* lacking three of the five *rpf*-like genes are defective for growth in vivo and for resuscitation in vitro. Infect. Immun. **73:**3038–3043.
12. **Dye, C., S. Scheele, P. Dolin, V. Pathania, and M. C. Raviglione.** 1999. Consensus statement. Global burden of tuberculosis: estimated incidence, prevalence, and mortality by country. WHO Global Surveillance and Monitoring Project. JAMA **282:**677–686.
13. **Dziarski, R.** 2003. Recognition of bacterial peptidoglycan by the innate immune system. Cell Mol. Life Sci. **60:**1793–1804.
14. **Flynn, J. L., C. A. Scanga, K. E. Tanaka, and J. Chan.** 1998. Effects of aminoguanidine on latent murine tuberculosis. J. Immunol. **160:**1796–1803.
15. **Glickman, M. S., J. S. Cox, and W. R. Jacobs, Jr.** 2000. A novel mycolic acid cyclopropane synthetase is required for cording, persistence, and virulence of *Mycobacterium tuberculosis*. Mol. Cell **5:**717–727.
16. **Hett, E. C., M. C. Chao, L. L. Deng, and E. J. Rubin.** 2008. A mycobacterial enzyme essential for cell division synergizes with resuscitation-promoting factor. PLoS Pathog. **4:**e1000001.
17. **Hett, E. C., M. C. Chao, A. J. Steyn, S. M. Fortune, L. L. Deng, and E. J. Rubin.** 2007. A partner for the resuscitation-promoting factors of *Mycobacterium tuberculosis*. Mol. Microbiol. **66:**658–668.
18. **Jacobs, C., J. M. Frere, and S. Normark.** 1997. Cytosolic intermediates for cell wall biosynthesis and degradation control inducible beta-lactam resistance in gram-negative bacteria. Cell **88:**823–832.
19. **Jacobs, C., L. J. Huang, E. Bartowsky, S. Normark, and J. T. Park.** 1994. Bacterial cell wall recycling provides cytosolic muropeptides as effectors for beta-lactamase induction. EMBO J. **13:**4684–4694.
20. **Jagannath, C., J. K. Actor, and R. L. Hunter, Jr.** 1998. Induction of nitric oxide in human monocytes and monocyte cell lines by *Mycobacterium tuberculosis*. Nitric Oxide **2:**174–186.
21. **Kana, B. D., B. G. Gordhan, K. J. Downing, N. Sung, G. Vostroktunova, E. E. Machowski, L. Tsenova, M. Young, A. Kaprelyants, G. Kaplan, and V. Mizrahi.** 2008. The resuscitation-promoting factors of *Mycobacterium tuberculosis* are required for virulence and resuscitation from dormancy but are collectively dispensable for growth in vitro. Mol. Microbiol. **67:**672–684.
22. **Kaushal, D., B. G. Schroeder, S. Tyagi, T. Yoshimatsu, C. Scott, C. Ko, L. Carpenter, J. Mehrotra, Y. C. Manabe, R. D. Fleischmann, and W. R. Bishai.** 2002. Reduced immunopathology and mortality despite tissue per-

sistence in a *Mycobacterium tuberculosis* mutant lacking alternative sigma factor, SigH. Proc. Natl. Acad. Sci. USA **99:**8330–8335.
23. **Keep, N. H., J. M. Ward, M. Cohen-Gonsaud, and B. Henderson.** 2006. Wake up! Peptidoglycan lysis and bacterial non-growth states. Trends Microbiol. **14:**271–276.
24. **Koraimann, G.** 2003. Lytic transglycosylases in macromolecular transport systems of Gram-negative bacteria. Cell Mol. Life Sci. **60:**2371–2388.
25. **Kurtz, S., K. P. McKinnon, M. S. Runge, J. P. Ting, and M. Braunstein.** 2006. The SecA2 secretion factor of *Mycobacterium tuberculosis* promotes growth in macrophages and inhibits the host immune response. Infect. Immun. **74:**6855–6864.
26. **Lavollay, M., M. Arthur, M. Fourgeaud, L. Dubost, A. Marie, N. Veziris, D. Blanot, L. Gutmann, and J. L. Mainardi.** 2008. The peptidoglycan of stationary phase *Mycobacterium tuberculosis* predominantly contains cross-links generated by L,D-transpeptidation. J. Bacteriol. **190:**4360–4366.
27. **MacMicking, J. D., R. J. North, R. LaCourse, J. S. Mudgett, S. K. Shah, and C. F. Nathan.** 1997. Identification of nitric oxide synthase as a protective locus against tuberculosis. Proc. Natl. Acad. Sci. USA **94:**5243–5248.
28. **Manca, C., M. B. Reed, S. Freeman, B. Mathema, B. Kreiswirth, C. E. Barry III, and G. Kaplan.** 2004. Differential monocyte activation underlies strain-specific *Mycobacterium tuberculosis* pathogenesis. Infect. Immun. **72:**5511–5514.
29. **Manca, C., L. Tsenova, S. Freeman, A. K. Barczak, M. Tovey, P. J. Murray, C. Barry, and G. Kaplan.** 2005. Hypervirulent *M. tuberculosis* W/Beijing strains upregulate type I IFNs and increase expression of negative regulators of the Jak-Stat pathway. J. Interferon Cytokine Res. **25:**694–701.
30. **McCune, R. M., Jr., and R. Tompsett.** 1956. Fate of *Mycobacterium tuberculosis* in mouse tissues as determined by the microbial enumeration technique. I. The persistence of drug-susceptible tubercle bacilli in the tissues despite prolonged antimicrobial therapy. J. Exp. Med. **104:**737–762.
31. **McCune, R. M., Jr., R. Tompsett, and W. McDermott.** 1956. The fate of *Mycobacterium tuberculosis* in mouse tissues as determined by the microbial enumeration technique. II. The conversion of tuberculous infection to the latent state by the administration of pyrazinamide and a companion drug. J. Exp. Med. **104:**763–802.
32. **McDonald, C., N. Inohara, and G. Nunez.** 2005. Peptidoglycan signaling in innate immunity and inflammatory disease. J. Biol. Chem. **280:**20177–20180.
33. **McKinney, J. D., K. Honer zu Bentrup, E. J. Munoz-Elias, A. Miczak, B. Chen, W. T. Chan, D. Swenson, J. C. Sacchettini, W. R. Jacobs, Jr., and D. G. Russell.** 2000. Persistence of *Mycobacterium tuberculosis* in macrophages and mice requires the glyoxylate shunt enzyme isocitrate lyase. Nature **406:**735–738.
34. **Medina, E., and R. J. North.** 1998. Resistance ranking of some common inbred mouse strains to *Mycobacterium tuberculosis* and relationship to major histocompatibility complex haplotype and Nramp1 genotype. Immunology **93:**270–274.
35. **Mohan, V. P., C. A. Scanga, K. Yu, H. M. Scott, K. E. Tanaka, E. Tsang, M. C. Tsai, J. L. Flynn, and J. Chan.** 2001. Effects of tumor necrosis factor alpha on host immune response in chronic persistent tuberculosis: possible role for limiting pathology. Infect. Immun. **69:**1847–1855.
36. **Mukamolova, G. V., A. S. Kaprelyants, D. I. Young, M. Young, and D. B. Kell.** 1998. A bacterial cytokine. Proc. Natl. Acad. Sci. USA **95:**8916–8921.
37. **Mukamolova, G. V., A. G. Murzin, E. G. Salina, G. R. Demina, D. B. Kell, A. S. Kaprelyants, and M. Young.** 2006. Muralytic activity of *Micrococcus luteus* Rpf and its relationship to physiological activity in promoting bacterial growth and resuscitation. Mol. Microbiol. **59:**84–98.
38. **Mukamolova, G. V., O. A. Turapov, D. I. Young, A. S. Kaprelyants, D. B. Kell, M. Young, K. Kazarian, and M. Telkov.** 2002. A family of autocrine growth factors in *Mycobacterium tuberculosis*. Mol. Microbiol. **46:**623–635.
39. **Munoz-Elias, E. J., J. Timm, T. Botha, W. T. Chan, J. E. Gomez, and J. D. McKinney.** 2005. Replication dynamics of *Mycobacterium tuberculosis* in chronically infected mice. Infect. Immun. **73:**546–551.
40. **North, R. J., and Y. J. Jung.** 2004. Immunity to tuberculosis. Annu. Rev. Immunol. **22:**599–623.
41. **Rao, V., N. Fujiwara, S. A. Porcelli, and M. S. Glickman.** 2005. *Mycobacterium tuberculosis* controls host innate immune activation through cyclopropane modification of a glycolipid effector molecule. J. Exp. Med. **201:**535–543.
42. **Rao, V., F. Gao, B. Chen, W. R. Jacobs, Jr., and M. S. Glickman.** 2006. Trans-cyclopropanation of mycolic acids on trehalose dimycolate suppresses *Mycobacterium tuberculosis*-induced inflammation and virulence. J. Clin. Investig. **116:**1660–1667.
43. **Reed, M. B., P. Domenech, C. Manca, H. Su, A. K. Barczak, B. N. Kreiswirth, G. Kaplan, and C. E. Barry III.** 2004. A glycolipid of hypervirulent tuberculosis strains that inhibits the innate immune response. Nature **431:**84–87.
44. **Reed, R. R.** 1981. Resolution of cointegrates between transposons gamma delta and Tn*3* defines the recombination site. Proc. Natl. Acad. Sci. USA **78:**3428–3432.
45. **Rees, R. J., and P. D. Hart.** 1961. Analysis of the host-parasite equilibrium in chronic murine tuberculosis by total and viable bacillary counts. Br. J. Exp. Pathol. **42:**83–88.
46. **Rich, E. A., M. Torres, E. Sada, C. K. Finegan, B. D. Hamilton, and Z. Toossi.** 1997. *Mycobacterium tuberculosis* (MTB)-stimulated production of nitric oxide by human alveolar macrophages and relationship of nitric oxide production to growth inhibition of MTB. Tuber. Lung Dis. **78:**247–255.
47. **Rickman, L., C. Scott, D. M. Hunt, T. Hutchinson, M. C. Menendez, R. Whalan, J. Hinds, M. J. Colston, J. Green, and R. S. Buxton.** 2005. A member of the cAMP receptor protein family of transcription regulators in *Mycobacterium tuberculosis* is required for virulence in mice and controls transcription of the *rpfA* gene coding for a resuscitation promoting factor. Mol. Microbiol. **56:**1274–1286.
48. **Rousseau, C., N. Winter, E. Pivert, Y. Bordat, O. Neyrolles, P. Ave, M. Huerre, B. Gicquel, and M. Jackson.** 2004. Production of phthiocerol dimycocerosates protects *Mycobacterium tuberculosis* from the cidal activity of reactive nitrogen intermediates produced by macrophages and modulates the early immune response to infection. Cell Microbiol. **6:**277–287.
49. **Royet, J., and J. M. Reichhart.** 2003. Detection of peptidoglycans by NOD proteins. Trends Cell Biol. **13:**610–614.
50. **Ruggiero, A., B. Tizzano, A. Geerlof, E. Pedone, C. Pedone, M. Wilmanns, and R. Berisio.** 2007. Expression, purification, crystallization and preliminary X-ray crystallographic analysis of a resuscitation-promoting factor from *Mycobacterium tuberculosis*. Acta Crystallogr. Sect. F **63:**870–873.
51. **Scanga, C. A., V. P. Mohan, H. Joseph, K. Yu, J. Chan, and J. L. Flynn.** 1999. Reactivation of latent tuberculosis: variations on the Cornell murine model. Infect. Immun. **67:**4531–4538.
52. **Scanga, C. A., V. P. Mohan, K. Tanaka, D. Alland, J. L. Flynn, and J. Chan.** 2001. The inducible nitric oxide synthase locus confers protection against aerogenic challenge of both clinical and laboratory strains of *Mycobacterium tuberculosis* in mice. Infect. Immun. **69:**7711–7717.
53. **Scanga, C. A., V. P. Mohan, K. Yu, H. Joseph, K. Tanaka, J. Chan, and J. L. Flynn.** 2000. Depletion of $CD4^+$ T cells causes reactivation of murine persistent tuberculosis despite continued expression of IFN-gamma and NOS2. J. Exp. Med. **192:**347–358.
54. **Seiler, P., T. Ulrichs, S. Bandermann, L. Pradl, S. Jorg, V. Krenn, L. Morawietz, S. H. Kaufmann, and P. Aichele.** 2003. Cell-wall alterations as an attribute of *Mycobacterium tuberculosis* in latent infection. J. Infect. Dis. **188:**1326–1331.
55. **Shimono, N., L. Morici, N. Casali, S. Cantrell, B. Sidders, S. Ehrt, and L. W. Riley.** 2003. Hypervirulent mutant of *Mycobacterium tuberculosis* resulting from disruption of the *mce1* operon. Proc. Natl. Acad. Sci. USA **100:**15918–15923.
56. **Singh, A., R. Gupta, R. A. Vishwakarma, P. R. Narayanan, C. N. Paramasivan, V. D. Ramanathan, and A. K. Tyagi.** 2005. Requirement of the *mymA* operon for appropriate cell wall ultrastructure and persistence of *Mycobacterium tuberculosis* in the spleens of guinea pigs. J. Bacteriol. **187:**4173–4186.
57. **Stanley, S. A., S. Raghavan, W. W. Hwang, and J. S. Cox.** 2003. Acute infection and macrophage subversion by *Mycobacterium tuberculosis* require a specialized secretion system. Proc. Natl. Acad. Sci. USA **100:**13001–13006.
58. **Stewart, G. R., V. A. Snewin, G. Walzl, T. Hussell, P. Tormay, P. O'Gaora, M. Goyal, J. Betts, I. N. Brown, and D. B. Young.** 2001. Overexpression of heat-shock proteins reduces survival of *Mycobacterium tuberculosis* in the chronic phase of infection. Nat. Med. **7:**732–737.
59. **Steyn, A. J., D. M. Collins, M. K. Hondalus, W. R. Jacobs, Jr., R. P. Kawakami, and B. R. Bloom.** 2002. *Mycobacterium tuberculosis* WhiB3 interacts with RpoV to affect host survival but is dispensable for in vivo growth. Proc. Natl. Acad. Sci. USA **99:**3147–3152.
60. **Tufariello, J. M., W. R. Jacobs, Jr., and J. Chan.** 2004. Individual *Mycobacterium tuberculosis* resuscitation-promoting factor homologues are dispensable for growth in vitro and in vivo. Infect. Immun. **72:**515–526.
61. **Tufariello, J. M., K. Mi, J. Xu, Y. C. Manabe, A. K. Kesavan, J. Drumm, K. Tanaka, W. R. Jacobs, Jr., and J. Chan.** 2006. Deletion of the *Mycobacterium tuberculosis* resuscitation-promoting factor Rv1009 gene results in delayed reactivation from chronic tuberculosis. Infect. Immun. **74:**2985–2995.
62. **Turner, J., M. Gonzalez-Juarrero, B. M. Saunders, J. V. Brooks, P. Marietta, D. L. Ellis, A. A. Frank, A. M. Cooper, and I. M. Orme.** 2001. Immunological basis for reactivation of tuberculosis in mice. Infect. Immun. **69:**3264–3270.
63. **Zahrt, T. C., and V. Deretic.** 2001. *Mycobacterium tuberculosis* signal transduction system required for persistent infections. Proc. Natl. Acad. Sci. USA **98:**12706–12711.
64. **Zignol, M., M. S. Hosseini, A. Wright, C. L. Weezenbeek, P. Nunn, C. J. Watt, B. G. Williams, and C. Dye.** 2006. Global incidence of multidrug-resistant tuberculosis. J. Infect. Dis. **194:**479–485.

Editor: F. C. Fang